



# Sub-50 ps pulses at 620 nm obtained from frequency doubled 1240 nm diamond Raman laser

JARI NIKKINEN,\* ANTTI HÄRKÖNEN, AND MIRCEA GUINA

*Optoelectronics Research Centre, Tampere University of Technology, Korkeakoulunkatu 3, 33720 Tampere, Finland*

*\*jari.nikkinen@tut.fi*

**Abstract:** We report a monolithic 1240 nm diamond Raman laser producing pulses with duration of 42–62 ps at 100 kHz repetition rate, and maximum average power of 246 mW. The Raman laser is formed by a 0.5-mm thick planar diamond, coated on both sides and pumped by ~100 ps pulses from a Q-switched 1064 nm laser. The maximum conversion efficiency from 1064 nm to 1240 nm was about 25%. The 1240 nm signal was frequency-doubled in single-pass configuration through a 10-mm long LBO crystal, enabling generation of pulses with a duration of 29–46 ps at 620 nm. The maximum average power at 620 nm was 128 mW, and the maximum conversion efficiency from 1240 nm to 620 nm was 50%. The Raman laser provides an efficient and flexible way to extend short pulse operation to wavelengths in spectral domains difficult to reach, such as 620 nm and in addition provides a simple pulse shortening mechanisms.

© 2017 Optical Society of America under the terms of the [OSA Open Access Publishing Agreement](#)

**OCIS codes:** (140.3538) Lasers, pulsed; (140.3550) Lasers, Raman; (140.7300) Visible lasers.

## References and links

1. B. Braun, F. X. Kärtner, G. Zhang, M. Moser, and U. Keller, "56-ps passively Q-switched diode-pumped microchip laser," *Opt. Lett.* **22**(6), 381–383 (1997).
2. E. Mehner, B. Bernard, H. Giessen, D. Kopf, and B. Braun, "Sub-20-ps pulses from a passively Q-switched microchip laser at 1 MHz repetition rate," *Opt. Lett.* **39**(10), 2940–2943 (2014).
3. G. J. Spühler, R. Paschotta, R. Fluck, B. Braun, M. Moser, G. Zhang, E. Gini, and U. Keller, "Experimentally confirmed design guidelines for passively Q-switched microchip lasers using semiconductor saturable absorbers," *J. Opt. Soc. Am. B* **16**, 376–388 (1999).
4. R. S. Balmer, J. R. Brandon, S. L. Clewes, H. K. Dhillon, J. M. Dodson, I. Friel, P. N. Inglis, T. D. Madgwick, M. L. Markham, T. P. Mollart, N. Perkins, G. A. Scarsbrook, D. J. Twitchen, A. J. Whitehead, J. J. Wilman, and S. M. Woollard, "Chemical vapour deposition synthetic diamond: materials, technology and applications," *J. Phys. Condens. Matter* **21**(36), 364221 (2009).
5. W. Lubeigt, G. M. Bonner, J. E. Hastie, M. D. Dawson, D. Burns, and A. J. Kemp, "Continuous-wave diamond Raman laser," *Opt. Lett.* **35**(17), 2994–2996 (2010).
6. R. J. Williams, O. Kitzler, A. McKay, and R. P. Mildren, "Investigating diamond Raman lasers at the 100 W level using quasi-continuous-wave pumping," *Opt. Lett.* **39**(14), 4152–4155 (2014).
7. R. P. Mildren, J. E. Butler, and J. R. Rabeau, "CVD-diamond external cavity Raman laser at 573 nm," *Opt. Express* **16**(23), 18950–18955 (2008).
8. S. Reilly, V. G. Savitski, H. Liu, E. Gu, M. D. Dawson, and A. J. Kemp, "Monolithic diamond Raman laser," *Opt. Lett.* **40**(6), 930–933 (2015).
9. D. J. Spence, E. Granados, and R. P. Mildren, "Mode-locked picosecond diamond Raman laser," *Opt. Lett.* **35**(4), 556–558 (2010).
10. J. Lin and D. J. Spence, "25.5 fs dissipative soliton diamond Raman laser," *Opt. Lett.* **41**(8), 1861–1864 (2016).
11. P. Černý, H. Jelínková, T. T. Basiev, and P. G. Zverev, "Highly efficient picosecond Raman generators based on the BaWO<sub>4</sub> crystal in the near infrared, visible, and ultraviolet," *IEEE J. Quantum Electron.* **38**(11), 1471–1478 (2002).
12. T. T. Basiev, P. G. Zverev, A. Ya. Karasik, V. V. Osiko, A. A. Sobol, and D. S. Chunaev, "Picosecond stimulated Raman scattering in crystals," *J. Exp. Theor. Phys.* **99**(5), 934–941 (2004).
13. A. A. Kaminskii, H. J. Eichler, K. Ueda, N. V. Klassen, B. S. Redkin, L. E. Li, J. Findeisen, D. Jaque, J. García-Sole, J. Fernández, and R. Balda, "Properties of Nd<sup>3+</sup>-doped and undoped tetragonal PbWO<sub>4</sub>, NaY(WO<sub>4</sub>)<sub>2</sub>, CaWO<sub>4</sub>, and undoped monoclinic ZnWO<sub>4</sub> and CdWO<sub>4</sub> as laser-active and stimulated Raman scattering-active crystals," *Appl. Opt.* **38**(21), 4533–4547 (1999).

14. A. A. Kaminskii, C. L. McCray, H. R. Lee, S. W. Lee, D. A. Temple, T. H. Chyba, W. D. Marsh, J. C. Barnes, A. N. Annanenkov, V. D. Legun, H. J. Eichler, G. M. A. Gad, and K. Ueda, "High efficiency nanosecond Raman lasers based on tetragonal PbWO<sub>4</sub> crystals," *Opt. Commun.* **183**(1–4), 277–287 (2000).
15. A. Penzkofer, A. Laubereau, and W. Kaiser, *High Intensity Raman Interactions* (Pergamon Press, 1979).
16. V. G. Savitski, S. Reilly, and A. J. Kemp, "Steady-state Raman gain in diamond as a function of pump wavelength," *IEEE J. Quantum Electron.* **49**(2), 218–223 (2013).
17. J. Nikkinen, A. Härkönen, I. Leino, and M. Guina, "Generation of sub-100 ps pulses at 532 nm, 355 nm and 266 nm using a SESAM Q-switched microchip laser," *IEEE Photonics Technol. Lett.* **29**(21), 1816–1819 (2017).
18. R. Mildren and J. Rabeau, *Optical Engineering of Diamond* (Wiley-VCH, 2013).
19. Y. R. Shen and N. Bloembergen, "Theory of stimulated Brillouin and Raman scattering," *Phys. Rev.* **137**(6A), A1787–A1805 (1965).
20. S. Ding, X. Zhang, Q. Wang, F. Su, S. Li, S. Fan, S. Zhang, J. Chang, S. Wang, and Y. Liu, "Theoretical models for the extracavity Raman laser with crystalline Raman medium," *Appl. Phys. B* **85**(1), 89–95 (2006).

## 1. Introduction

Picosecond optical pulses are instrumental for a number of applications in science, metrology, industrial processing and defense. While the 1–30 ps pulse region is dominated by mode locked lasers, longer 250 ps – 100 ns pulse region is covered by simpler Q-switched lasers. The development of SESAM Q-switched microchip lasers at 1064 nm, has enabled generation of pulses with duration below 100 ps [1], and recently even down to 16 ps [2], already overlapping with the traditional mode locked pulse regime. The main advantages of Q-switched microchip platform compared to mode locked laser system include simpler laser design, potentially lower cost, but in particular the ability to operate at low, sub-MHz repetition rates and pulse energies in  $\mu\text{J}$  range or higher. These are key parameters for many applications, but hard to achieve with mode locked lasers, without active pulse picking and stages of power amplification, which add to the cost and complexity.

The short pulse Q-switched microchip lasers typically combine a semiconductor saturable absorber mirror (SESAM) used as the Q-switching element [3] and high emission cross section Nd:YVO<sub>4</sub> gain material, allowing shortest possible cavity length and thus minimizing the pulse duration. The gain element and SESAM can form a monolithic plane–plane laser resonator, which is stabilized by a thermal lens, avoiding the need for any external laser mirrors requiring precise alignment.

In this work, a Q-switched 1064 nm microchip master-oscillator power-amplifier (MOPA) system is used for pumping a 1240 nm diamond Raman laser. The Raman lasers are highly appealing devices as they enable frequency conversion to longer wavelengths than the input (pump), and allow access to wavelengths that are difficult to reach by direct laser emission or by harmonic generation. Diamond is an ideal Raman laser gain material due to its high Raman gain [4], excellent thermal conductivity and wide transparency range. To date, diamond Raman lasers have been demonstrated as intra- and external-cavity continuous wave pumped lasers [5, 6], Q-switched nanosecond [7, 8] and mode locked [9, 10] femtosecond and picosecond lasers. Moreover, picosecond Raman output has been achieved by pumping Raman generators [11, 12] and Raman lasers [13, 14] with high energy (mJ) mode locked picosecond pump lasers. The ultimate target of our work was to demonstrate a practical, sub-100 ps, 620 nm laser source with  $>1 \mu\text{J}$  pulse energy and narrow spectral width suitable for time-gated Raman spectroscopy application.

In principle, the 620 nm emission could be generated either by frequency-doubling 1240 nm signal (1st Stokes line of 1064 nm pump), or alternatively by generating 2nd Stokes emission from 532 nm pump signal. The higher Raman gain at the visible wavelengths [15, 16] could favor the latter option. However, optimization of the mirror reflectivity is easier for only one Stokes wavelength (1240 nm), and at the same time it is possible to suppress any other Stokes lines and thus concentrate most of the energy at the targeted Stokes wavelength.

## 2. Experimental and results

The experimental system, shown in Fig. 1, included the 1064 nm pump source, the Raman diamond, a half-wave plate, an LBO frequency-doubling crystal, a 620/1240 nm dichroic mirror, and focusing/collimating optics.

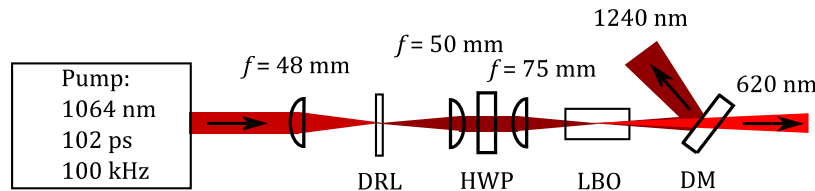


Fig. 1. A schematic presentation of the setup. DRL: diamond Raman laser, HWP: half-wave plate, LBO: lithium triborate, DM: dichroic mirror.

The pump consisted of a SESAM Q-switched Nd:YVO<sub>4</sub> microchip master-oscillator and a 6-mm long Nd:YVO<sub>4</sub> bulk amplifier. The system produced ~100 ps pulses at 1064 nm, with spectral width of 0.075 nm, 100 kHz repetition rate and, ~1 W average power. The pulse energy was therefore about 10 μJ and the peak power >100 kW. The details of the pump setup are described in [17].

The diamond Raman laser consisted of a 0.537-mm thick (100)-polished single crystal diamond (MB optics BV), which was coated on both sides to form a plane–plane resonator. The pump input coating was highly transmissive for the 1064 nm pump signal and high reflective for the 1240 nm 1st Stokes emission. The output coupler coating was high reflective at 1064 nm, to enable double-pass pumping, and about 51% reflective for the 1240 nm 1st Stokes line. Both coatings were designed to be highly transmissive ( $R \sim 3\%$  and  $\sim 1.2\%$ ) for the 2nd Stokes line at 1486 nm, in order to minimize emission at any higher order Stokes. The dephasing time of a diamond is about 7 ps [18]. Thus, the ratio of pump pulse duration and the dephasing time is about 15. Therefore, the gain is near the limit of steady-state case, see Fig. 17 of [15].

The pump was focused with an  $f = 48$  mm lens to a 30/50 μm diameter spot (horizontal/vertical) on the Raman diamond, which was kept at near 0° tilt angle, incident to the pump beam. The pump was linearly polarized at direction of lowest threshold pump power, but its orientation in regard to the crystal axis of the diamond was not known.

The generated 1240 nm Raman signal was collimated and focused to a 10-mm long lithium triborate (LBO) nonlinear crystal, which was critically phase-matched (type I,  $\theta = 85.8^\circ$ ,  $\varphi = 0^\circ$ ) and stabilized to 25 °C temperature using a peltier element. The LBO crystal was anti-reflection coated on both sides at 1240–1260 nm and 620–630 nm wavelengths. The Raman laser output was linearly polarized and a half-wave plate was used prior to the LBO crystal to adjust the orientation of the polarization for proper phase-matching. The fundamental (1240 nm) and harmonic (620 nm) signals were spatially separated using a dichroic mirror.

The measurements of the diamond Raman laser and the frequency-doubling were carried out separately and they were characterized for output power, pulse width, spectra, and beam profile. The output power was measured with a thermal power meter (Ophir Optronics 3W), the pulse width with a Femtochrome FR-103WS autocorrelator, the spectra with optical spectrum analyzers (ANDO AQ6317C and Yokogawa AQ6373), and the beam profiles with a PyroCam and a CCD beam profiler.

Output power characteristics and the conversion efficiency of the diamond Raman laser are presented in Fig. 2(a). Lasing threshold was achieved at average power of 395 mW, corresponding to an incident threshold peak intensity of about 3 GW/cm<sup>2</sup>. A maximum of 246 mW of output power was achieved with a conversion efficiency of 25% with the output

power being limited by the available pump power. Typical autocorrelation traces are shown in Fig. 3(a), and the pulse durations at different output powers are presented in Fig. 3(b). The pulse duration was found to change from ~42 ps at low pump power to 62 ps at maximum pump power. This tendency can be explained by the nonlinear operation principle of the Raman laser: At low pump power, the Raman laser can exceed its lasing threshold only for a short period of time when the pump pulse intensity is sufficiently high. At higher pump powers the threshold will be reached earlier, leading to longer Raman pulse and increased conversion efficiency. The 1240 nm output spectrum is presented in Fig. 2(b) and has a spectral width of 0.057 nm, which is slightly narrower than the 0.075 nm width of the pump signal.

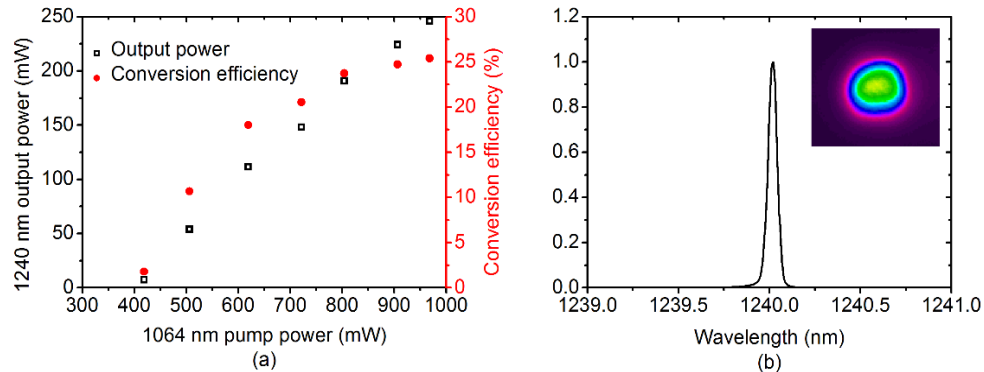


Fig. 2. (a) Diamond Raman laser average output power and conversion efficiency to the 1240 nm 1st Stokes line and (b) Output spectrum of the diamond Raman laser at 1240 nm. Inset: Beam profile of the 1240 nm output.

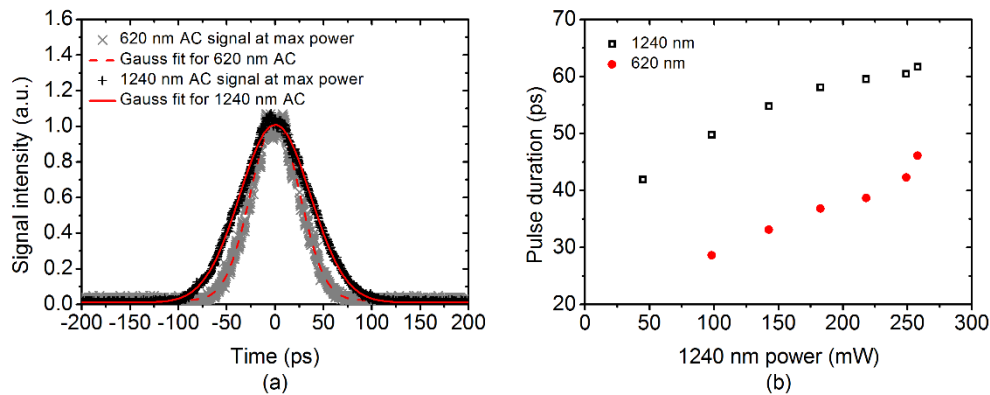


Fig. 3. (a) Typical autocorrelation trace of the 1240 nm diamond Raman laser output with Gaussian fit and (b) measured pulse durations at 1240 nm and 620 nm, given as a function of 1240 nm output power. The 1240 nm pulse duration was measured separately from 620 nm frequency doubling.

At high pump powers, altogether three Stokes and three anti-Stokes emission lines were observed. However, the combined average power of the 2nd (1486 nm) and 3rd (1852 nm) Stokes lines was less than 10 mW, while the combined power of the anti-Stokes emission was in the range of tens or hundreds of  $\mu\text{W}$ . The spectra of all observed Stokes and anti-Stokes lines are presented in Fig. 4. The higher order Stokes emission could possibly be reduced by more optimized coatings, but due to the high optical intensity in the Raman gain medium, some amount of higher order Stokes and anti-Stokes emission will always be present in the system [19].

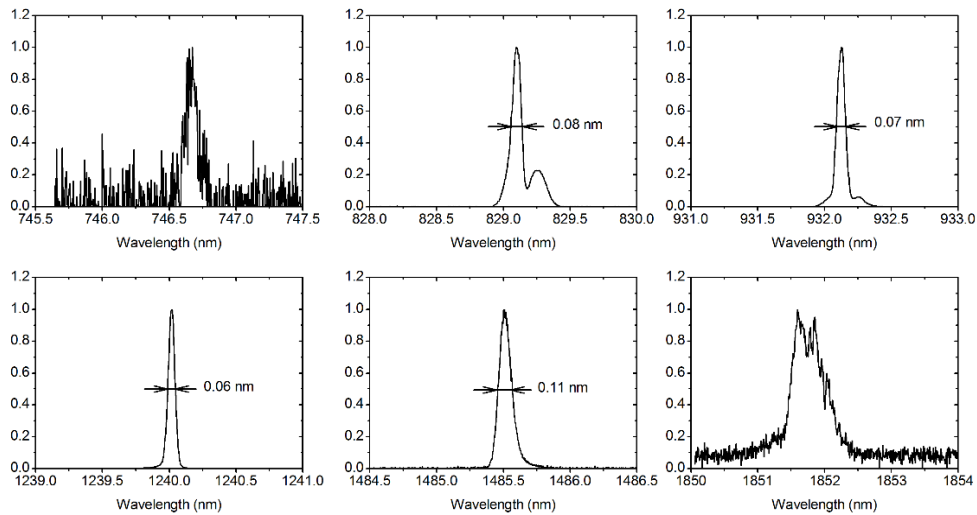


Fig. 4. Measured Raman laser output spectra including 1st–3rd anti-Stokes and 1st–3rd Stokes lines. Intensities are normalized.

The Raman laser output was passed through the LBO frequency doubling crystal and the generated 620 nm emission was measured as a function of the input power. The 620 nm output characteristics are shown in Fig. 5(a) with the corresponding conversion efficiency. At maximum, 128 mW of 620 nm average output was achieved with a conversion efficiency of 50%. Typical autocorrelation traces are shown in Fig. 3(a). The pulse width at 620 nm followed similar trend as the input pulse, and increased from ~29 ps at low power to 46 ps at the maximum power, see Fig. 3(b). The spectrum of the 620 nm output is shown in Fig. 5(b). The measured spectral width was about 0.11 nm.

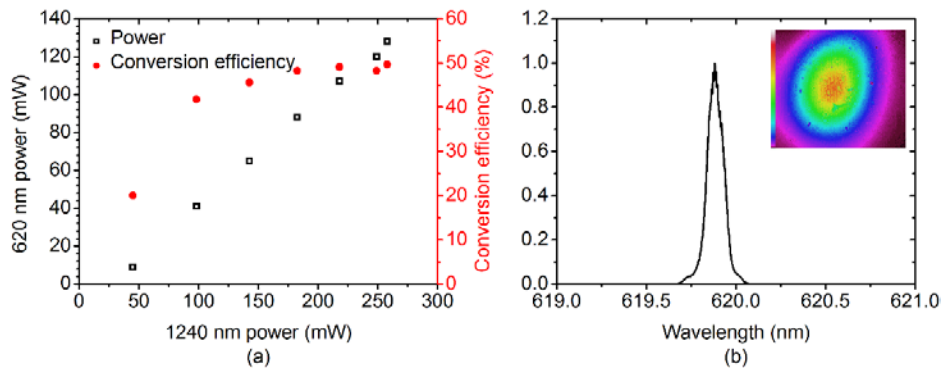


Fig. 5. (a) Average power and the conversion efficiency of the 620 nm frequency doubled output and (b) spectrum of the 620 nm output. Inset: Beam profile of the 620 nm output.

The overall efficiency achieved in this work from 1064 nm pump to 620 nm was 12.5%. Emission at 620 nm could be also achieved by first frequency doubling the 1064 nm to 532 nm and then Raman shifting the 532 nm to 2nd Stokes line. Typical conversion efficiencies of frequency doubled 532 nm are about ~50%, and so to reach the same overall efficiency, the conversion efficiency from 532 nm to 2nd Stokes 620 nm line should be 25%, which to date has not been reported with such short Q-switched pulses. Moreover, the conversion efficiency to 1240 nm could be improved by further optimizing the diamond thickness, pump spot diameter and the output coupler reflectivity [20]. Use of periodically-poled nonlinear crystals for frequency doubling could also increase the overall efficiency.

### 3. Conclusion and future outlook

In conclusion, we have demonstrated a compact laser system, which can produce 46 ps picosecond pulses at 620 nm wavelength. Up to 128 mW of average power was achieved at 100 kHz repetition rate, yielding 1.28  $\mu$ J of pulse energy, and 26 kW peak power. Such combination of low repetition rate, picosecond pulse width, and high pulse energy is very difficult to achieve at reasonable cost, as most mode locked lasers operate intrinsically at much higher repetition rates and require high-power amplifier stages while picosecond diode lasers are not able to produce high pulse energies. Overall, the 570–630 nm wavelength range is extremely challenging for diode lasers due to limitations of semiconductor materials.

The obtained results suggest that the future work could include generation of sub-50 ps pulses at 310 nm UV wavelength by adding another stage of single-pass frequency-doubling to the system. Also by redesigning the Raman laser mirrors, it should be possible to generate sufficient amounts of 1486 nm 2nd Stokes emission with sub-100 ps pulse duration. Such laser could be used for high-resolution eye-safe LIDAR, for example. By further frequency-doubling one could also generate 743 nm emission, which closely matches with the spectral region currently accessed by alexandrite lasers.

#### Funding

Academy of Finland (282431)

#### Acknowledgment

We would like to acknowledge valuable help and discussions with Prof. Alan Kemp's group from the University of Strathclyde, Glasgow, Scotland.